



**HAL**  
open science

## Monitoring discharge in a tidal river using water level observations: Application to the Saigon River, Vietnam

B. Camenen, N. Gratiot, J.-A. Cohard, F. Gard, V.Q. Tran, A.-T. Nguyen,  
Guillaume Dramais, T. van Emmerik, J. Némery

### ► To cite this version:

B. Camenen, N. Gratiot, J.-A. Cohard, F. Gard, V.Q. Tran, et al.. Monitoring discharge in a tidal river using water level observations: Application to the Saigon River, Vietnam. *Science of the Total Environment*, 2021, 761, pp.1-12. 10.1016/j.scitotenv.2020.143195 . hal-03118389

**HAL Id: hal-03118389**

**<https://hal.science/hal-03118389v1>**

Submitted on 22 Jan 2021

**HAL** is a multi-disciplinary open access archive for the deposit and dissemination of scientific research documents, whether they are published or not. The documents may come from teaching and research institutions in France or abroad, or from public or private research centers.

L'archive ouverte pluridisciplinaire **HAL**, est destinée au dépôt et à la diffusion de documents scientifiques de niveau recherche, publiés ou non, émanant des établissements d'enseignement et de recherche français ou étrangers, des laboratoires publics ou privés.

# Monitoring discharge in a tidal river using water level observations: application to the Saigon River, Vietnam

B. Camenen<sup>a,\*</sup>, N. Gratiot<sup>b,c</sup>, J.-A. Cohard<sup>b</sup>, F. Gard<sup>b</sup>, V. Q. Tran<sup>b,c</sup>, A.-T. Nguyen<sup>b,c</sup>, G. Dramais<sup>a</sup>, T. van Emmerik<sup>d</sup>, J. Némery<sup>b,c</sup>

<sup>a</sup>*Inrae, UR RiverLy, centre de Lyon-Grenoble, Villeurbanne, France*

<sup>b</sup>*CARE, IRD, Ho-Chi-Minh-City, Vietnam*

<sup>c</sup>*IGE, Univ. Grenoble Alpes / CNRS / IRD / Grenoble INP, Grenoble, France*

<sup>d</sup>*HQWM, Univ. Wageningen, Wageningen, The Netherlands*

---

## Abstract

The hydrological dynamics of the Saigon River is ruled by a complex combination of factors, which need to be disentangled to prevent and limit risks of flooding and salt intrusion. In particular, the Saigon water discharge is highly influenced by tidal cycles with a relatively low net discharge. This study proposes a low-cost technique to estimate river discharge at high frequency (every 10 minutes in this study). It is based on a stage-fall-discharge (SFD) rating curve adapted from the general Manning Strickler law, and calibrated thanks to two ADCP campaigns. Two pressure sensors were placed at different locations of the river in September 2016: one at the centre of Ho Chi Minh City and one in Phu Cuong, 40 km upstream approximately. The instantaneous water discharge data were used to evaluate the net residual discharge and to highlight seasonal and inter-annual trends. Both water

---

\*Corresponding author, benoit.camenen@inrae.fr

level and water discharge show a seasonal behaviour. Rainfall, including during the Usagi typhoon that hit the megalopolis in November 2018, has no clear and direct impact on water level and water discharge due to the delta flat morphology and complex response between main channel and side channel network and ground water in this estuarine system under tidal influence. However, we found some evidences of interactions between precipitation, groundwater, the river network and possibly coastal waters. This paper can be seen as a proof of concept to (1) present a low-cost discharge method that can be applied to other tidal rivers, and (2) demonstrate how the high-frequency discharge data obtained with this method can be used to evaluate discharge dynamics in tidal river systems.

*Keywords:* Saigon River, water level, water discharge, tidal river, flood, stage-fall-discharge rating curve.

---

## 1. Introduction

A good understanding of the hydrological cycle, and discharge in particular, in tidal rivers enables reliable forecasting and decision making by researchers and policy makers. Some priorities are generally put on the protections against floods, saline intrusion and the dynamics of pollutants because of the social, economic and political stakes they are linked to. Hydrological cycles in Low Elevation Coastal (and deltaic) Zone (LECZ, 0-10 masl) differ

8 a lot from their upstream environments due to the tidal influence ([van Driel](#)  
9 [et al., 2015](#)). Although this is a strategic zone at the interface between land  
10 and ocean, physical and environmental data collected in this environment re-  
11 main sparse because of inherent logistical difficulties due to the unsteadiness  
12 of the flow ([Taniguchi et al., 2013](#)). On one hand, the river water discharge  
13 is influenced by tidal dynamics, which modulate hydrodynamics at high and  
14 low frequency and can reshape the geomorphology, with feedback loops on  
15 hydrodynamics ([Mao et al., 2004](#)). On the other hand, estuarine and deltaic  
16 zones are highly influenced by peak fresh water discharges, which are them-  
17 selves modulated by tidal asymmetry ([Sassi and Hoitink, 2013](#)).

18 In the floodplain of the Saigon River, which is part of the LECZ of the  
19 south of Vietnam, vulnerability could be assessed according to four factors  
20 ([McGranahan et al., 2007](#); [van Driel et al., 2015](#)) : (i) Relative Sea Level Rise  
21 (RSLR) due to climate change and natural and anthropogenic subsidence;  
22 (ii) Wetland ecological threat; (iii) Population pressure: and (iv) Delta gov-  
23 ernance (adaptivity, participation, fragmentation). The Saigon River flows  
24 through Ho Chi Minh City (HCMC), a highly populated area, where popu-  
25 lation density can reach up to 30,000 inhabitants/km<sup>2</sup> ([Nguyen et al., 2019](#)).  
26 The unprecedented growth of HCMC induces pressure on the environment  
27 and especially water resources ([Van Leeuwen et al., 2016](#)).

28 A major issue in such regions is to measure the instantaneous discharge

29 for a tidal river and to evaluate the residual discharge of the tide-affected  
30 river. Indeed, a simple stage-discharge relationship cannot be used because  
31 of the downstream influence of the tide. Stage-fall-discharge (SFD) rating  
32 curves are traditionally and successfully used to compute discharge at sites  
33 where variable backwater effects could affect a classical stage-discharge re-  
34 lationship (Rantz, 1982). Such methods have recently improved thanks to  
35 Bayesian methods (Petersen-Overleir and Reitan, 2009; Mansanarez et al.,  
36 2016). However, the relation between stage, slope, and discharge has gen-  
37 erally been considered too complex in tidal rivers to attempt to obtaining  
38 accurate discharges. Rantz (1963) proposed a graphical method using mul-  
39 tiple correlation, which remains difficult to apply, especially when the tidal  
40 influence leads to discharge fluctuations as large as the residual discharge.  
41 That is the reason why there exists nearly no hydrometric stations world-  
42 wide in such rivers. Recently, acoustic sensing techniques (through HADCP,  
43 Horizontal Acoustic Doppler Current Profiler) have been implemented suc-  
44 cessfully in some tidal rivers such as the Sacramento River, California (Ruhl  
45 and DeRose, 2004) or in the rivers Berau and Mahakam in East Kaliman-  
46 tan, Indonesia (Hoitink et al., 2009; Sassi et al., 2011). Such techniques  
47 generally correspond to a velocity index method. Similar method using an  
48 ADP (Acoustic Doppler Profiler) current meter was deployed on the Tan-  
49 shui River, Taiwan (Chen et al., 2012b) or fixed ADCPs (Acoustic Doppler

50 Current Profiler) on the Yangtze River at Xuliujing, China (Zhao et al.,  
51 2016; Mei et al., 2019). These methods remain however expensive (around  
52 30k€excluding structural works and maintenance) and difficult to display in  
53 an urban place due to risk of vandalism.

54 In a recent work, Camenen et al. (2017) proposed to apply a stage-fall-  
55 discharge rating curve to estimate instantaneous discharges in tidal rivers.  
56 Such simple model can be calibrated using intense discharge campaigns achieved  
57 over a full tide cycle, which are easily available nowadays thanks to the ADCP  
58 technology. The first application of the method was based on field measure-  
59 ments made on the Saigon River in September 2016 and was particularly  
60 successful (Camenen et al., 2017). It presented some limitations for a very  
61 asymmetric tidal wave (close to a tidal bore), which is not the case for the  
62 Saigon River.

63 In this paper, this simple low-cost water level-based discharge monitoring  
64 is applied the Saigon River for a two-year period. A calibration and validation  
65 of the method are first presented. The monitoring of two hydrological seasons  
66 from January 2017 to Dec 2019 is then discussed. Results obtained allow for  
67 examining and discussing two specific aspects : first, what is the hydrological  
68 pattern of the Saigon River at different time scales, from the event scale to  
69 years, and how is it influenced by the sea level ; second, how much the rainfall  
70 regime is directly influencing the Saigon River dynamics, in particular, how

71 does the river react to extreme events?

## 72 **2. Material and methods**

### 73 *2.1. Study site*

74 The Saigon River is located in the South of Vietnam, in a low elevation  
75 coastal zone, i.e. between 0 and 10 m above mean sea level (MSL, Figure  
76 1). The Saigon River takes its source in Cambodia and is 225 km long.  
77 Its catchment area has a surface of 4717 km<sup>2</sup> (Nguyen et al., 2019). The  
78 Saigon River is actually a complex river system, subject to several human  
79 and environmental interactions, including many canals while it crosses Ho  
80 Chi Minh City (HCMC) megalopolis, before flowing into the Dong Nai River  
81 and the coastal waters. Upstream the megalopolis, the river is regulated by  
82 the Dau Tieng dam, which was built during the 1980's, in order to mitigate  
83 saline intrusion and secure the fresh water supply uptake station of HCMC.  
84 The situation of HCMC is all the more critical as 65% of the city is located  
85 at an altitude of 1.5 m above MSL (Scussolini et al., 2017; Vachaud et al.,  
86 2019).

87 The flow of the Saigon River is predominantly driven by tidal currents,  
88 which affects both the water level and water discharge, with regular exfil-  
89 tration of water in some urban districts during high spring tides. Over the  
90 year, precipitation follow two contrasted seasons: the dry season, usually ex-

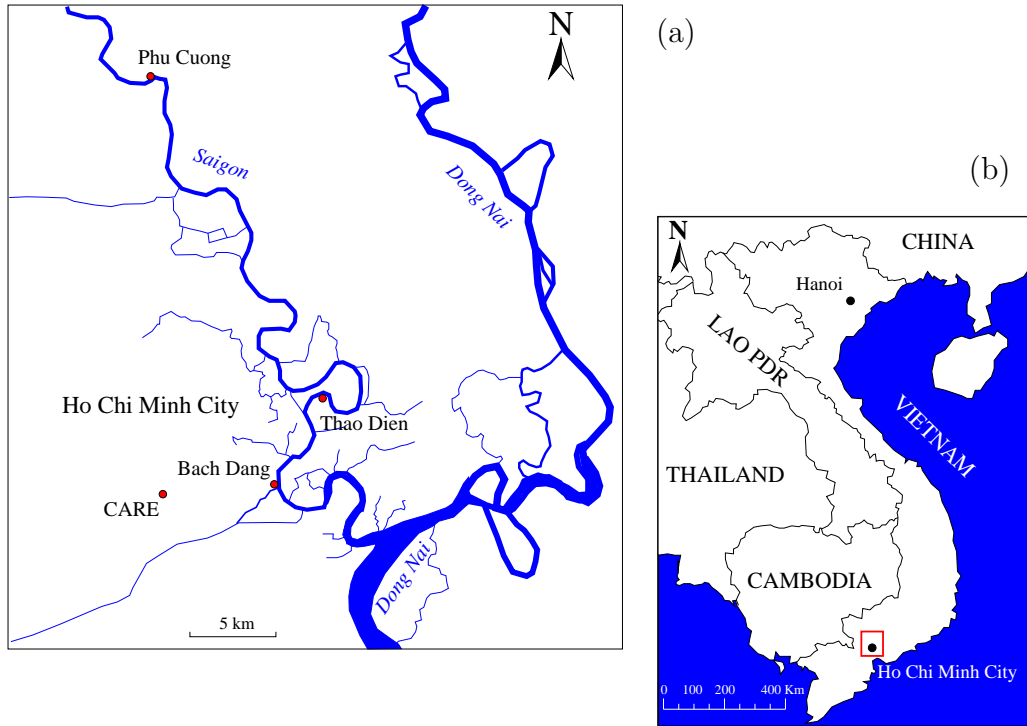


Figure 1: Location of the study site: the low elevation coastal zone of the Saigon River system, including the Saigon and Dong Nai rivers and Ho Chi Minh City (red points correspond to the position of pressure gauges).

91 tending from November to April and the wet season from May to October,  
 92 which gathers about 80% of the total rain (Nguyen et al., 2019). Rain event  
 93 can be severe and precipitation record can locally exceed 300 mm/day, even  
 94 400 mm/day. In this paper, we focus on one of the most severe rainy events  
 95 that experienced the city. It occurred in November 2018, when Usagi typhoon  
 96 hit HCMC. During this event, there was an increase of more than 300 mm  
 97 in rainfall which caused flooding, material and human damages reported in



98 several newspapers.

## 99 2.2. Water discharge estimation

100 The instantaneous water discharge was estimated by applying a stage-fall-  
101 discharge (SFD) rating curve adapted from the general Manning-Strickler  
102 law, previously tested and validated by [Camenen et al. \(2017\)](#). This model  
103 is based on the assumption of a pseudo-uniform flow and a prismatic sec-  
104 tion, which is valid for a low slope river with slowly varying water depth.  
105 Considering an almost constant flow between two water level measures, the  
106 Manning-Strickler equation can be applied :

$$Q = K A_w R_h^{2/3} \sqrt{S} \quad (1)$$

107 with  $Q$  the water discharge [ $\text{m}^3/\text{s}$ ],  $K$  the Manning-Strickler coefficient [ $\text{m}^{1/3}/\text{s}$ ],  
108  $R_h = A_w/P_w$  the hydraulic radius [ $\text{m}$ ],  $A_w$  the wet section [ $\text{m}^2$ ],  $P_w$  the wet  
109 perimeter [ $\text{m}$ ], and  $S$  the energy slope [-] assumed equal to the water slope.  
110 Another assumption made here is that the river section and reach are stable  
111 with no significant bed changes. It was verified by comparing the different  
112 bathymetries from both ADCP campaigns.

113 Two hydrological stations are needed to evaluate the hydraulic slope of  
114 the river: the water level  $z_{up}$  and  $z_{dn}$  were measured at Phu Cuong (upstream  
115 station) and Bach Dang then Thao Dien stations (downstream stations),  
116 which are named “PC”, “BD”, and “TD” hereafter (see Fig. 1a). Distance

117 between stations is around  $L = 42$  km (PC-BD) and  $L = 35$  km (PC-TD),  
 118 which is sufficient to have a significant difference in altitude and to estimate  
 119 slope with a good resolution for this low slope system. Due to tides and  
 120 flow oscillation, the slope oscillates between positive and negative values.  
 121 Also, the slope in Equation (1) ( $S = (z_{up} - z_{dn})/L$ ) does not correspond to  
 122 the local slope at the point in which the discharge is evaluated, i.e. at Phu  
 123 Cuong (PC). Indeed, because of the distance between the two stations, the  
 124 flow discharge is slightly different at the two stations. However, this spatial  
 125 offset can be translated as a lag time  $\Delta t$ . As a consequence, the discharge  
 126 estimation at PC can be written :

$$Q(t) = K A_w(z_{up}(t)) R_h(z_{up}(t))^{2/3} \sqrt{|S(t + \Delta t)|} \frac{S(t + \Delta t)}{|S(t + \Delta t)|} \quad (2)$$

127 By specifying the river cross-section at PC (assuming it is relevant for the  
 128 whole reach), one can easily evaluate  $A_w$  and  $R_h$  as a function of the water  
 129 level  $z_{up}$ . In Equation (2), two parameters need to be calibrated :

- 130 -  $K$ , the Strickler coefficient of the river reach supposed homogeneous  
 131 between PC and BD,
- 132 -  $\Delta t$ , a priori negative since the tide progresses from downstream to  
 133 upstream.

134 The Strickler coefficient could vary depending on the discharge due to addi-  
 135 tional head losses at low flows (emergence of sills) or at high flows (flood-plain

136 interaction). Nevertheless, such cases were not observed for the specific case  
137 of the Saigon River.

### 138 *2.3. Water level measurement*

139 To apply Equation (2), CTD DIVER sensors were installed at PC and BD  
140 stations in September 2016, as reported in Figure 1. They measure pressure,  
141 conductivity and temperature every 10 minutes. Conductivity and temper-  
142 ature were considered as interesting proxy to interpret data series and were  
143 used to operate the post processing, but were not used directly in this study.  
144 PC sensor was immersed in the river bank of the Saigon River, close to Phu  
145 Cuong city, TD sensor was immersed in the heart of the megalopolis of Ho  
146 Chi Minh City, in Thao Dien district. Both sensors were downloaded at a  
147 bimonthly basis. Due to logistical constraints, significant risks of theft and  
148 of mechanical deterioration, TD station was displaced twice with a corre-  
149 sponding adjustment of parameters in Equation (2) ( $L$  and  $\Delta t$ ). The sensor  
150 was initially installed in Bach Dang, in the city centre in September 2016. It  
151 was moved to Boat House (BH), 8.5 km upstream of the Bach Dang point,  
152 from January 2017 to the 8th of March 2017. Then, since 15th March 2017,  
153 the sensor is located in Thao Dien Village (TD). Distance between those  
154 two last sites is only 0.9 km. To compensate water level measurements from  
155 atmospheric pressure fluctuations, a barometer was installed at the CARE

156 center (Ho Chi Minh University of Technology, see Figure 1).

157 Some drifts of the water level measurements were observed due to fine  
158 deposit accumulation leading to over-pressure. Water levels at PC and TD  
159 were thus corrected based on monthly campaigns made by Sub Institute  
160 of Hydrometeorology and Climate Change (SIHYMECC, also named CEM  
161 hereafter for Center of Environmental Monitoring) of Ho Chi Minh City.  
162 During these campaigns, water levels were measured every hour for three  
163 days at the staff gauge. In Figure 2, one can observed a very good agreement  
164 between CTD DIVER data and SIHYMECC data (the water level  $H$  cor-  
165 responds the the difference between the water surface level and a reference  
166 level of the station).

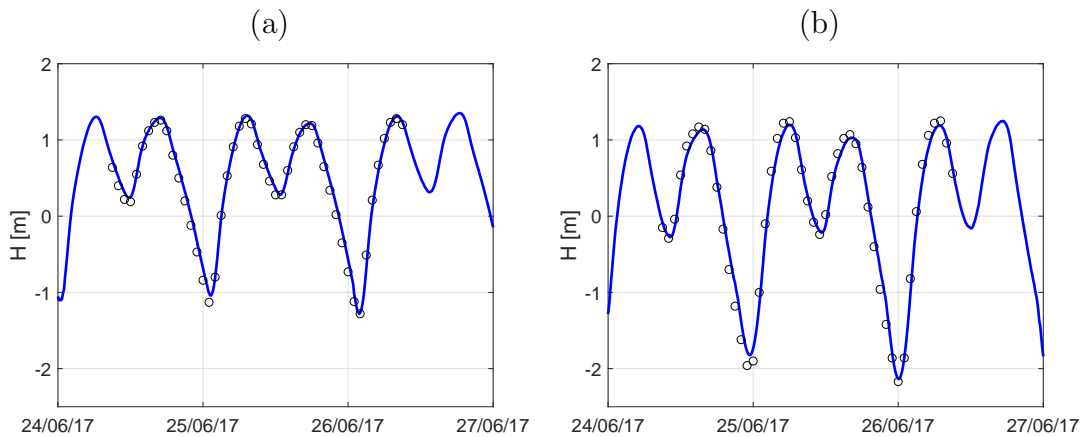


Figure 2: Comparison between water levels  $H$  measured at PC (a) and TD (b) stations and water levels measured by the SIHYMECC at the staff gauges for the selected period between 24th to 27th of June 2017.

167 *2.4. Residual discharge*

168 In order to study the net water discharge in the Saigon River and eval-  
169 uate the hydrological cycle, the instantaneous water discharge needs to be  
170 averaged over four tide periods ( $T_{tide} = 12.4$  hours) to filter the 1st order  
171 semi-diurnal tidal signal from the data-series. As a consequence,  $Q_n(t_0) =$   
172  $\int_{t_0-2T_{tide}}^{t_0+2T_{tide}} Q(t)dt$ . In the same way, the tidal averaged water level can be ob-  
173 tained such as  $z_{ta}(t_0) = \int_{t_0-2T_{tide}}^{t_0+2T_{tide}} z(t)dt$ . The acquisition of data at high  
174 frequency (every 10 minutes) and over a longer period (two hydrological sea-  
175 sons) is a prerequisite to such evaluation.

176 **3. Calibration and validation of the SFD rating curve**

177 *3.1. Calibration of the model using ADCP campaigns*

178 Two Acoustic Doppler Current Profiler (ADCP) campaigns have been led  
179 in September 2016 and March 2017 with a Rio Grande 600 kHz ([Dinehart](#)  
180 [and Burau, 2005](#)). During 24 hours and for every hour, one gauging, i.e.  
181 three transects, was realized at PC with a boat and a georeferenced ADCP  
182 mounted on it. ADCP campaigns were used to calibrate the water discharge  
183 estimation, calculated with Equation (2) ([Camenen et al., 2017](#)).  $K$  and  
184  $\Delta t$  were calibrated such as the modelled discharge fit to observed data (see  
185 also appendix [Appendix A.1](#)). Also, since it is very difficult to evaluate the  
186 exact vertical reference level of each station, these campaigns were used to

187 optimize the measured difference  $z_{up} - z_{dn}$  using an additional parameter  $\Delta z$   
188 (i.e.  $z_{up} - z_{dn} = (z_{up} - z_{dn})_{measured} + \Delta z$ )

189 To ensure the robustness of the hydraulic model, calibration were real-  
190 ized during both wet (September 2016) and dry (March 2017) seasons. These  
191 ADCP campaigns were also used to determine the river cross-section char-  
192 acteristics, to calculate  $A_w$  and  $R_h$  as a function of water level. Error in  
193 ADCP measurements were evaluated at 10% using a minimum error value of  
194  $100 \text{ m}^3/\text{s}$  since the conditions were adverse (Le Coz et al., 2016). We found  
195 the best results using a Manning-Strickler coefficient  $K = 26 \text{ m}^{1/3}/\text{s}$  and  
196  $\Delta t = -2.0$  hours (see Appendix [Appendix A.1](#)). Results are presented in  
197 [Fig. 3](#). Very good results can be observed for the September 2016 campaign.  
198 Some slight error may be observed at the end of the first flow peak ([Fig.](#)  
199 [3a](#), at around 21 h, local time) but it is due to a pressure gauge outside  
200 water. For the 2017 campaign, results are not as accurate but still in good  
201 agreement with data. The clear asymmetric semi-diurnal tidal signal for this  
202 specific day may explain some of the differences (Camenen et al., 2017).

### 203 *3.2. Validation of the model using other discharge estimations*

204 The monthly campaigns made by SIHYMECC also include some dis-  
205 charge estimation every hour for 48 h. They applied the velocity index  
206 method by measuring the water level and the depth-averaged velocity  $\overline{u_{index}}$

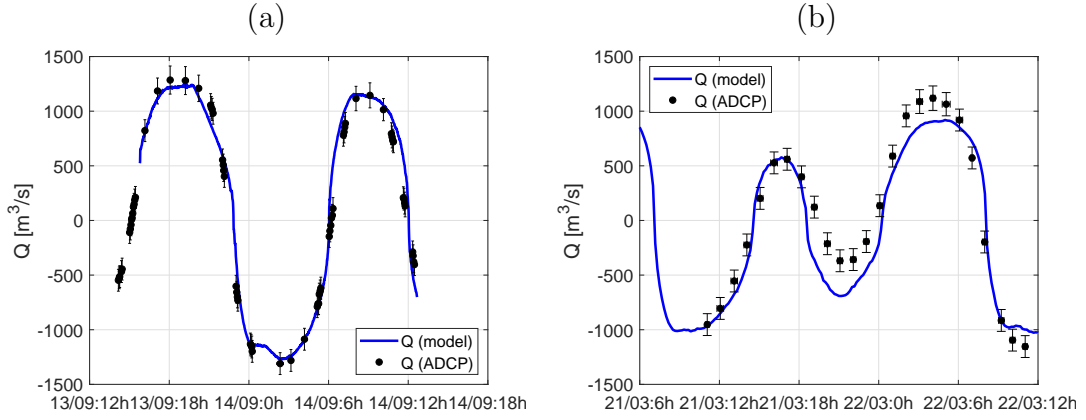


Figure 3: Water discharge  $Q$  comparison between model results and ADCP measurement campaigns in September 2016 (a) and March 2017 (b).

207 at one location  $y_{index}$  (Chen et al., 2012b) :

$$Q = \alpha_{index} \overline{u_{index}} A_w \quad (3)$$

208 with  $\alpha_{index} = 0.8$  a calibration coefficient,  $\alpha_{index} = U / \overline{u_{index}}$  where  $U = Q / A_w$   
 209 the section-averaged velocity. Again, since conditions are adverse, we roughly  
 210 estimated the error from this method equal to 15% plus a minimum error of  
 211 150 m<sup>3</sup>/s based on Ruhl and Simpson (2006).

212 The corresponding water discharge estimated from Equation (2) are in  
 213 good agreement with data from SIHYMECC (Fig. 4). The model tends to  
 214 yield smaller peak values for the inward discharge (negative), even if this  
 215 trend is not observed for all tidal cycles. This tendency is more pronounced  
 216 for the 2018 data (Fig. 4b). This could be the consequence of either a  
 217 varying flow repartition throughout the river section during the ebb and flow

218 not caught by the index velocity method or a bias on the slope estimation  
 219 by the proposed model based on a slope downstream of the station.

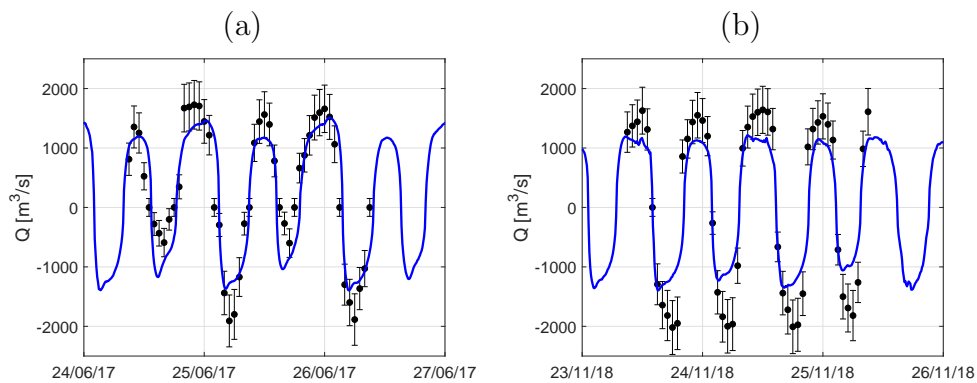


Figure 4: Water discharge  $Q$  estimated at PC (blue line) in comparison to SI-HYMECC data for two contrasting hydrological periods in June 2017 (a) and in November 2018 (b).

## 220 4. A two-year monitoring of the Saigon River

### 221 4.1. Water levels

222 The water level time series, which covers two hydrological years, from  
 223 January 2017 to December 2018 are reported in Figure 5a. For both stations,  
 224 the reference level is the one of the staff gauge, which explains the existence  
 225 of some negative values.

226 In each panel, one can see that the tidal signal clearly predominates with  
 227 a strong semi-diurnal harmonic. The cyclicity is particularly emphasized  
 228 through the examination of a zoomed period in September 2018 (Figure



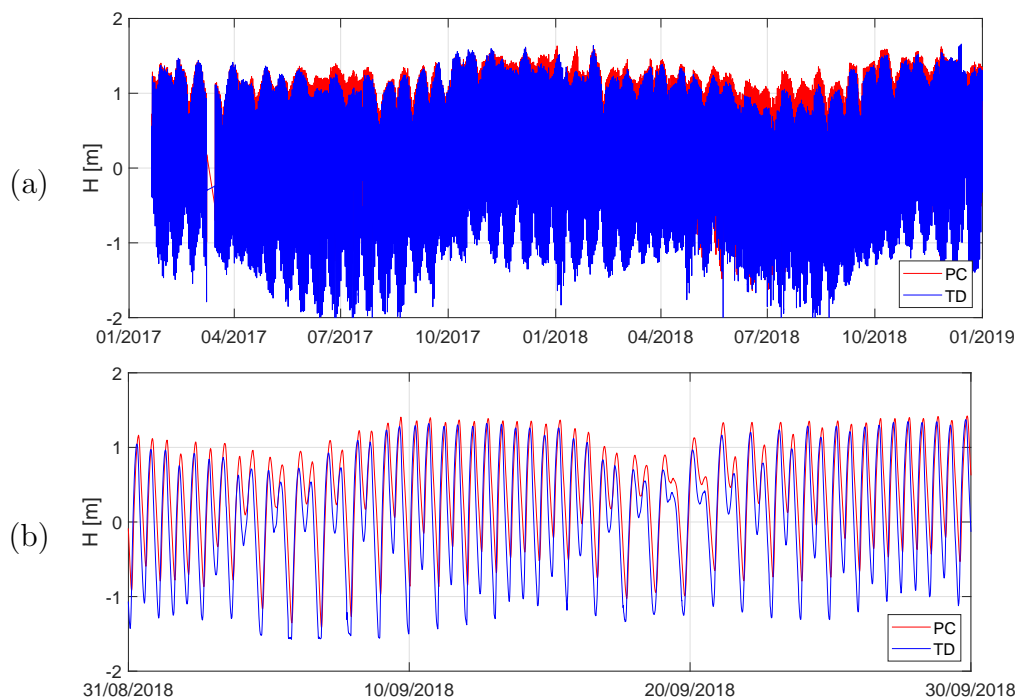


Figure 5: Two-year water level time series measured at PC and TD (a) with a zoom in September 2018 (b).

229 5b). The cyclicity is evidenced on both PC and TD stations, who present  
 230 synchronous fluctuations, with a time laps of about 1 hour and 10 minutes,  
 231 which corresponds to the duration of tide wave propagation between the two  
 232 stations. The tidal magnitude is smaller at PC station (by 17%) than at TD  
 233 station, which is physically consistent with quadratic friction dissipation: the  
 234 further upstream the station is, the less it is influenced by tidal waves. Tidal  
 235 range was measured to oscillate between -2.00 m and 1.50 m at both TD and  
 236 PC stations.

237 A first glimpse of seasonality can be observed in the two-year time-series.

238 One can observe lower water levels in the rainy season (May to September)  
239 and higher values in the dry season (November to March). Semi-diurnal tidal  
240 forcing clearly prevails on the Saigon River. As illustrated in Figures 2 and 5,  
241 the 14-days cycle presented both symmetric and asymmetric tides; a pattern  
242 which is particularly well developed in the estuaries located in the south of  
243 Vietnam (Chen et al., 2012b).

#### 244 4.2. Continuous discharge estimation

245 By applying Equation (2), one can easily calculate the discharge at PC  
246 using water levels from both PC and TD stations. Water discharge is domi-  
247 nated by tidal semi-diurnal harmonics, as for water level data-series (Figure  
248 6). Instantaneous discharge ranged from -2000 to 2000 m<sup>3</sup>/s. The oscilla-  
249 tion of the magnitude of tides, between spring and neap tides, is also well-  
250 identified (Figure 6b). Maxima appears at every syzygy between the sun, the  
251 moon and the earth. Overall, the analysis of instantaneous water discharge  
252 highlighted the predominant forcing of tides on any other forcing, despite  
253 contrasted and well-marked dry and rainy seasons.

#### 254 4.3. Residual discharge

255 All data from the SIHYMECC field campaigns (which correspond to a  
256 48 h experiment  $\approx 4T_{tide}$ ) were compared to the proposed model (Figure 7a).  
257 As expected, since the model yields smaller amplitudes (see Figure 4), one

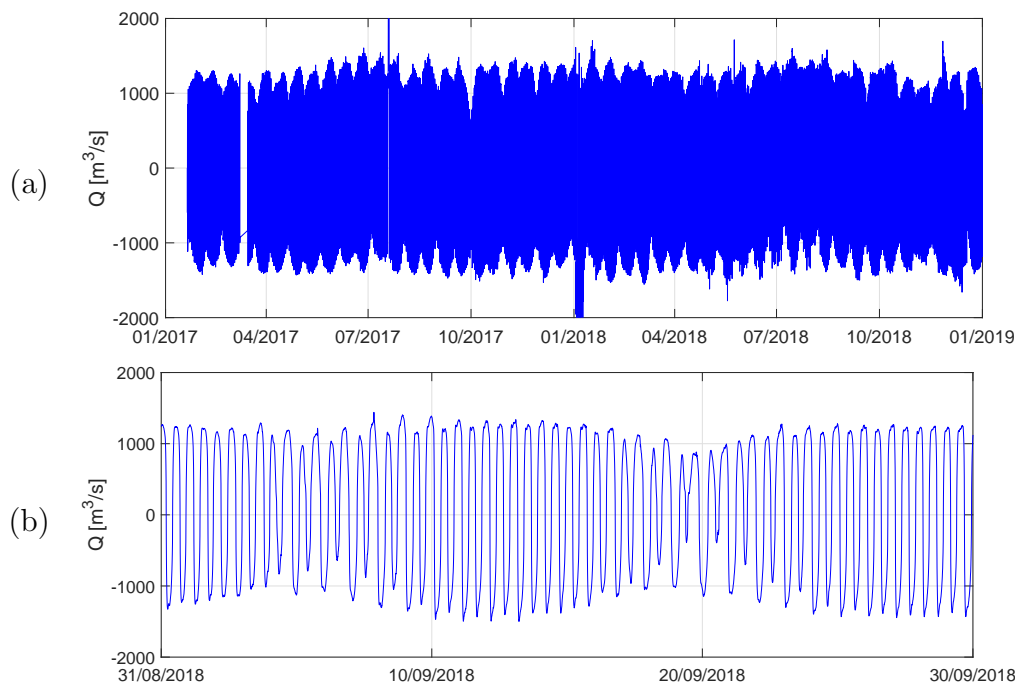


Figure 6: Two-year water discharge time-series (a) with a zoom in September 2018 (b) at Phu Cuong (PC).

258 generally finds a good correlation but with few outliers, predominantly above  
 259 the 1:1 line for negative discharge and below the 1:1 line for positive discharge  
 260 (i.e.  $|Q_{model}| \sim |Q(CEM)|$ ). One should note also the many zero values for  
 261 the SIHYMECC (CEM) data, which may be the consequence of a human bias  
 262 (while reading the staff gauge) and partly explains uncertainties in experi-  
 263 mental data and some of the scatter in the model response. A comparison of  
 264 the net water discharge measured by the SIHYMECC and modelled by our  
 265 group is reported in Figure 7b for the 18 SIHYMECC campaigns available.  
 266 One can realize the order of magnitude of difference between maximum in-

stantaneous discharges and net discharges, which corresponds to the red box  
in Figure 7a. Despite the existence of few outliers, modelled points for net  
water discharge are well correlated with the estimation from measured data.  
As expected, since the model yields smaller amplitudes, the net discharge  
estimations are generally smaller. The existence of outliers is not surpris-  
ing looking at the sensitivity of such calculation while net discharge is one  
order of magnitude smaller than peak values (positive and negative). But  
surprisingly, while SIHYMECC estimations of the net discharge are always  
positive, the proposed model leads sometimes to negative values. Although  
difficult to explain, these negative values may results from a combination of  
factors, such a the asymmetrical tides and complex exchanges with ground-  
water and with the canal network. The regular occurrence of salt intrusions  
up to HCMC does confirm the possible occurrence of a net negative water  
discharge. Also, as discussed above, the model is very sensitive to a possible  
error in water level estimation a PC and BD, TD stations. Hence, for the  
net discharge, we evaluated the error equal to  $20 \text{ m}^3/\text{s}$  per cm of error in the  
vertical axis (See Appendix [Appendix A.3](#)).

The net discharge time series over this two-year experiment is presented in  
Figure 8. Compared to monthly SIHYMECC campaigns, we observe more  
variability in the net discharge time-series. Some spikes are however not  
realistic and result from data gaps (January 2018, December 2019).

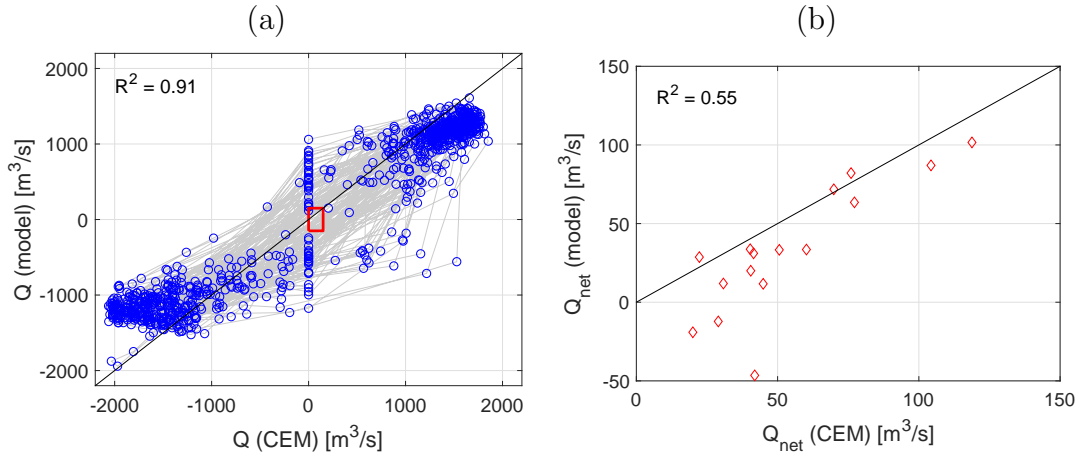


Figure 7: Comparison of the instantaneous (a) and net (b) discharges obtained by the SIHYMECC (CEM) and the proposed model for all 2017 and 2018 SIHYMECC campaigns.

288 The seasonality of precipitation in this tropical humid low lying area  
 289 is expectedly a main driver of the annual hydrological cycle, but as shown  
 290 previously, this driver is masked by the tidal forcing (Figure 8). The wet  
 291 season is expectedly linked with a higher water discharge and a refill of  
 292 the groundwater. At the opposite, the dry season is expectedly linked with  
 293 a decrease of the net water discharge. This general pattern was broadly  
 294 described by [Nguyen et al. \(2019\)](#), but needs to be detailed and should be  
 295 understood on a physically based characterization of the main drivers. One  
 296 can clearly observe the seasonality of net discharge with peak values during  
 297 the wet season in Figure 8. In 2017, the peak net discharge reached  $300 \text{ m}^3/\text{s}$   
 298 and lasted only for two months in the beginning of June and the end of

299 July. In 2018, net discharges exceeded  $200 \text{ m}^3/\text{s}$  from June to August with  
 300 maximum values up to  $400 \text{ m}^3/\text{s}$ . It then decreased before a second peak  
 301 was reached in early October. Flood extended for more than four months,  
 302 leading to one of the most humid year of the decade (Fig. 8 and Fig. 10).

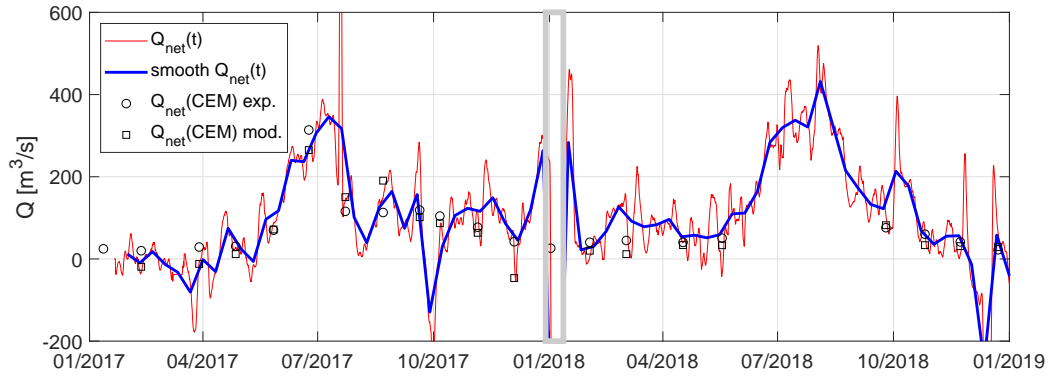


Figure 8: Net discharge  $Q_{net}$  estimate for the January 2017 - December 2019 period (full lines correspond to the model results while symbols correspond to values for the SIHYMECC campaigns using their own estimations -exp.- or using the model -mod.-; the grey line delimits a period of missing data at PC).

303 Monthly cumulated precipitation, tide-averaged water level along the  
 304 Saigon and Dong Nai rivers and monthly averaged net-discharge are pre-  
 305 sented in Figure 9 for the 2017 and 2018 periods. 2017 and 2018 rainy  
 306 seasons are well-marked, with an increase in precipitation from June to Oc-  
 307 tober. In 2018, precipitations are particularly high and extended in October  
 308 and November. The tide-averaged water level follows the rain pattern for  
 309 both increasing and decreasing phases, with a shift of two to three months.

310 Concerning the averaged water discharge, it was measured to fluctuate be-  
311 tween -100 to 500 m<sup>3</sup>/s (no value is given for January 2018 since there was a  
312 too long gap in data), with a magnitude that was quite different for both hy-  
313 drological years. In 2017, one can noticed that there exists an expected time  
314 lag between rain (first) and river discharge (few weeks later) but there is also  
315 some delayed and complex interactions with groundwater and/or water level.  
316 The rainy season, which started in May, was followed by a rise in the net  
317 water discharge only one month later (June) and then, by an increase of the  
318 tide-averaged water level few weeks later (July, August). Also, one observed  
319 a drop in net discharge in August and September, while precipitation remains  
320 high followed by a rise in net discharge while precipitation dropped. It seems  
321 there are strong exchanges of water with groundwater and/or floodplain with  
322 a possible recharge from the groundwater and/or floodplain in May, August  
323 and September and a restitution to the river in November and December.  
324 However, [Van and Koontanakulvong \(2018\)](#) estimated possible exchanges of  
325 water between the aquifer and the Saigon River of approximately 0.02 m<sup>3</sup>/s  
326 per km, which appears negligible. Effects of the large drainage and canal  
327 system around the Saigon River (i.e. of the Saigon floodplain) may prevail  
328 here. Also, anthropogenic influences such as Dau Tieng dam management  
329 or water supply pumping may significantly affect the net Saigon river water  
330 discharge. In 2018, cumulated rain also led to an increase of the net water

331 discharge, but the rise of the Saigon River discharge was much faster and  
332 almost correlated to precipitation, which lets presume that soil saturation  
333 was higher and led to a direct response of the river to precipitation. Even  
334 if rain initiated late in the season, as compared with year 2017 (May and  
335 June in 2018 instead of April and May in 2017), the shape and cumulative  
336 rain during the rainy season was quite comparable to 2017. The net water  
337 discharge responded similarly to 2017 in June 2018. However, in 2018 the  
338 response to precipitation is stronger with a monthly averaged net discharge  
339 above  $400 \text{ m}^3/\text{s}$  in July and August. Surprisingly, in October and November,  
340 while precipitation is particularly high in fall and superimposed with the ex-  
341 treme typhoon event in late November, one can observe a decrease of the net  
342 discharge. Significant floods have been observed during this period; a large  
343 part of the water volume from precipitation may have been spread over the  
344 flood plain.

345 Looking at the tide-averaged water level (Figure 9b) measured at Phu  
346 Cuong (PC), Thao Dien (TD) or Phu An (PA), but also at Vam Sat (station  
347 located downstream on the Dong Nai River at approximately 20 km from the  
348 see shore), a clear annual fluctuation can be observed with high water levels  
349 from October to April. Such high values yield an averaged negative slope  
350 leading some counter-effects on the net discharge (see Appendix [Appendix](#)  
351 [A.3](#)). Interestingly, these fluctuations are not correlated to precipitations



352 and could partially explain the deficit in net water discharge compared to  
 353 precipitation. We suspect these fluctuations to be a consequence of the peak  
 354 flow season of the Mekong River, which occurs in October in coastal flood-  
 355 plain and could influence sea water levels next to its river mouth (Chen et al.,  
 356 2012a; Ho et al., 2014; Thi Ha et al., 2018).

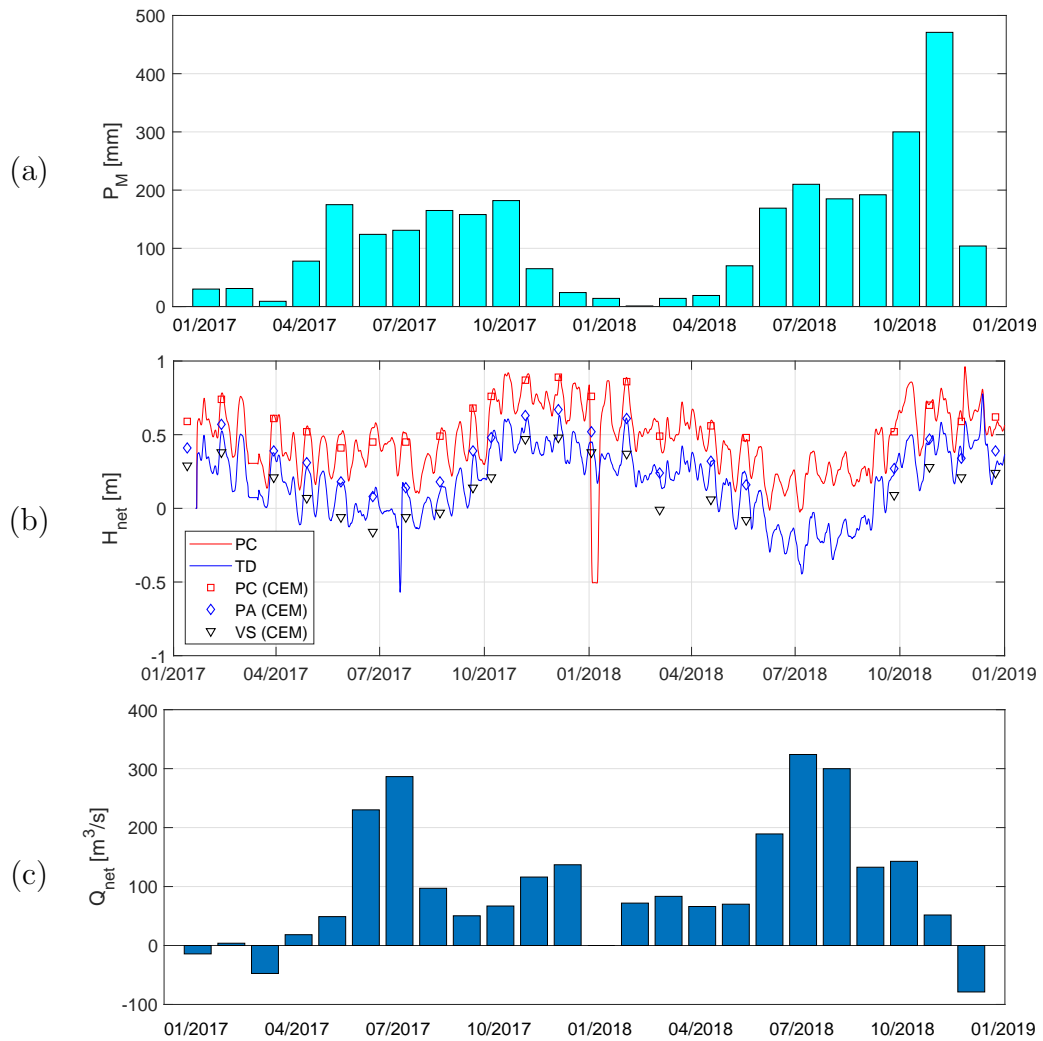


Figure 9: Monthly rainfall  $P_M$  (a), tide-averaged water levels  $H_{net}$  (b) and monthly net discharge  $Q_{M,net}$  (c) for the January 2017 - December 2019 period.

357 4.4. *Effects of long-term precipitation*

358 To get further in the analysis of the interaction between the Saigon River  
359 discharge and its surrounding floodplain, we examined a pluriannual monthly  
360 rainfall series (Figure 10). This series was associated with the severe Niño  
361 event in 2015-2016 (Thirumalai et al., 2017; Thi Ha et al., 2018). In Figure  
362 10, one can observed a regular decrease of annual precipitation from 2009  
363 to 2012, a minimum from 2013 to 2015 and an increase until 2019. The  
364 2013-2015 period thus corresponded to a deficit of rain, which was evidenced  
365 by socio-political impacts described in newspapers, particularly during the  
366 dry season 2015-2016. This dry season was reported as the worst drought  
367 ever reported in 98 years of monitoring in the floodplains of Mekong and  
368 Saigon-Dong Nai hydrosystems.

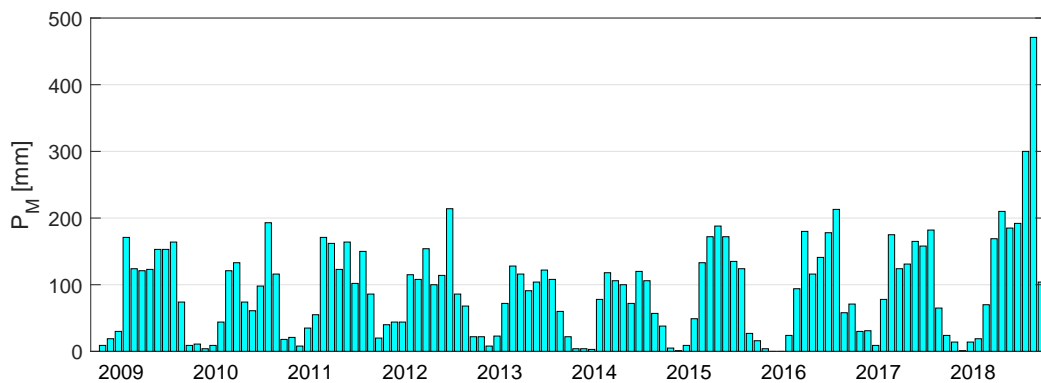


Figure 10: Monthly rainfall  $P_M$  at HCMC from 2009 to 2019.

369 The 2017-2018 and 2018-2019 hydrological seasons that are reported in  
370 Figure 9 support the hypothesis of a phase of recovery after these pluri-annual

371 droughts. The 2017 wet season showed a priori an atypical hydrological  
372 response, with a normal rainy season from May to October, that is not in  
373 correlation with water discharge due to strong exchanges with groundwater.  
374 There is indeed a shift between the discharge increase and the precipitation  
375 increase. This may result of years of deficit in the groundwater.

376 In 2018, the precipitation-river interaction was noticeably different. It  
377 seems the groundwater recovered from the drought leading to a more typical  
378 response of the river to precipitation. We may hypothesize that regional  
379 recovery of rain during the last wet seasons (2016-2018) led to a recharge  
380 of the groundwater table, and further of the river, presumably because the  
381 floodplain had fully recovered from the pluri-annual drought that hit the  
382 region from 2013 to 2016.

#### 383 *4.5. Effects of an extreme event : the Usagi typhoon*

384 On November 25th 2018, HCMC was hit by Usagi typhoon. Arriving from  
385 the East-south east, it reached the coast, at 50 km of Ho Chi Minh City (Ba  
386 Ria-Vung Tau Province) in the morning. It continued moving Northwest  
387 ward inland over HCMC area as a tropical depression. According to the  
388 forecast department of the Southern Centre for Hydro-Meteorological Fore-  
389 casting (SCHMF), this was the highest ever recorded rainfall in a 24-hours  
390 period in the megalopolis. Districts of HCMC recorder cumulated daily rain

391 between 293 to 408 mm for independent stations of measurements. While  
392 there is no debate concerning the intensity of Usagi event and the severity  
393 of damages, there is a clear interest in understanding how the hydrosystem  
394 physically behaved during and just after those exceptional rains. The para-  
395 doxical result is the lack of direct response of the Saigon River to the extreme  
396 precipitations. As shown in Figure 5, none of the two hydrological stations  
397 recorded any consistent rise of the water level during the typhoon, neither  
398 any flash rise of the river discharge (Figure 6). The only noticeable impact  
399 recorded by our CTD sensors was a slight reduction of the conductivity at  
400 the PC station, which dropped of a few percent when Usagi typhoon hit the  
401 region (not shown in this paper). Could we conclude that the typhoon had  
402 no effects on the river dynamics? Has the Dau Tieng dam totally regulated  
403 the flow?

404 By comparing data from November 2017 and November 2018, one can  
405 observe that despite a rise of rainfall by a factor six, mean water level and net  
406 discharge reduced during this period by 15% (0.77 m in Nov. 2017 and 0.66 m  
407 in Nov. 2018) and 50% ( $65 \text{ m}^3/\text{s}$  in Nov. 2017 and  $30 \text{ m}^3/\text{s}$  in Nov. 2018),  
408 respectively. It clearly shows that floods observed in some districts of the  
409 city during the event were not directly driven by the overflow of water from  
410 the river, but certainly by intense run off over impervious streets (Figure ??).  
411 Also, we should not underestimate the potential impact of the Dau Tieng

412 dam management; large amount of water may have been retained during the  
413 flood and slowly reinjected in the river during the following weeks. Finally,  
414 since tide-average water levels in the Saigon River are relatively higher in  
415 late fall (Fig. 9), and because of the storm surge, evacuation of water may  
416 have been more difficult. This can be explained by the morphology of the  
417 delta, which is very flat and close to the sea shore. Results from [Scussolini](#)  
418 [et al. \(2017\)](#) showed the influence of the sea level on HCMC flood risk. [Ho](#)  
419 [et al. \(2014\)](#) argued that main hydrological explanations for the flood risk  
420 on HCMC area are the upstream floods including those of the Dong Nai and  
421 Mekong delta, local rainfall, land subsidence, and sea level rise. Our results  
422 indicate that local rainfall and sea water level may be the most impacting  
423 factors.

## 424 5. Conclusion

425 Tidal rivers and their floodplains are environments that are hardly moni-  
426 tored although they concentrate most of the human activities and form habi-  
427 tats for rich ecosystems. Flood risk is a particular issue for such environment  
428 and requires a good monitoring and a good understanding of its hydrological  
429 functioning.

430 Here, we applied a stage-fall-discharge rating curve adapted from the gen-  
431 eral Manning-Strickler law ([Camenen et al., 2017](#)) to assess the instantaneous

432 water discharge on the Saigon River. For the first time, the Saigon River dy-  
433 namics was recorded at high frequency over two hydrological years, including  
434 the heaviest rain event ever recorded. Such tool appears to be a very effi-  
435 cient and low cost system for estimating discharge in tidal rivers as soon as  
436 the tidal wave is not too asymmetric and the river bed is stable (no general  
437 erosion nor aggradation). One issue remains the estimation of the slope since  
438 the model is sensitive to possible errors in water level measurements. This is  
439 particularly true for the Saigon River, which is tide dominated.

440     The analysis of the data-series highlights the driving role of tides on water  
441 mixing and water dynamics at hourly to monthly timescales. Once filtered  
442 from tidal effects, the averaged water level and water discharge points out a  
443 rather small contribution of run-off and a potential significant impact of flood  
444 plain and anthropogenic structures (Dau Tieng dam, canals, water pumping,  
445 etc.) to the hydrosystem response. The study of river response during Usagi  
446 typhoon illustrated how much the floodplain can attenuate the direct impact  
447 of intense precipitations and how critical is the sea water level to evacuate  
448 the flood. Also, the seasonal variability of the tidal-averaged water levels  
449 showed a possible influence of the nearby Mekong high flows that reduces  
450 the slope and limits the net discharge.

451     This study remains a preliminary study, which needs to be completed with  
452 some further studies on groundwater and flood plain dynamics, including

453 the complex canal network in HCMC to get an accurate evaluation of the  
454 vulnerability of the megalopolis to flooding during extreme events and how  
455 this vulnerability will evolve during coming decades under a worrying context  
456 of subsidence and sea level rise.

#### 457 *Acknowledgements*

458 This study was supported by the Rhône-Alpes region through the CMIRA  
459 Coopera financial support. We also wish to thank all the interns who worked  
460 on that topic throughout the last two years : Rémi Saillard, Lucas Barbieux,  
461 Roman Smoliakov and Swann Benaksas, as well as everyone involved in the  
462 two 24 hours field campaigns, which made the calibration possible. We are  
463 grateful to Dr. Nguyen Phuoc Dan from CARE center (HCMUT) and Dr  
464 Nguyen Van Hong from the sub-institute of hydrometeorology and climate  
465 change center (SIHYMECC) for providing us the field measurements of water  
466 level and water discharges.

#### **References**

Camenen, B., Dramais, G., Le Coz, J., Ho, T.-D., Gratiot, N., and Piney, S.  
(2017). Estimation d'une courbe de tarage hauteur-dénivelée-débit pour  
une rivière influencée par la marée. *La Houille Blanche*, 5:16–21. (in  
French).

- Chen, C., Lai, Z., Beardsley, R. C., Xu, Q., Lin, H., and Viet, N. T. (2012a). Current separation and upwelling over the southeast shelf of Vietnam in the South China Sea. *Journal of Geophysical Research*, 117(C03033):1–16.
- Chen, Y.-C., Yang, T.-M., Hsu, N.-S., and Kuo, T.-M. (2012b). Real-time discharge measurement in tidal streams by an index velocity. *Environmental Monitoring & Assessment*, 184:6423–6436.
- Dinehart, R. L. and Burau, J. R. (2005). Repeated surveys by acoustic Doppler current profiler for flow and sediment dynamics in a tidal river. *Journal of Hydrology*, 314(1-4):1–21.
- Ho, L. P., Nguyen, T., Chau, N. X. Q., and Nguyen, K. D. (2014). Integrated urban flood risk management approach in context of uncertainties: case study Ho Chi Minh city. *La Houille Blanche*, 6:26–33.
- Hoitink, A. J. F., Buschman, F. A., and Vermeulen, B. (2009). Continuous measurements of discharge from a horizontal acoustic Doppler current profiler in a tidal river. *Water Resources Research*, 45(11 ( W1140)):1–13.
- Le Coz, J., Blanquart, B., Pobanz, K., Dramais, G., Pierrefeu, G., Hauet, A., and Despax, A. (2016). Estimating the uncertainty of streamgauging techniques using in situ collaborative interlaboratory experiments. *Journal of Hydraulic Engineering*, 509:573–587.



- Mansanarez, V., Le Coz, J., Renard, B., Lang, M., Pierrefeu, G., and Vauchel, P. (2016). Bayesian analysis of stage-fall-discharge rating curves and their uncertainties. *Water Resources Research*, 52:7424–7443.
- Mao, Q., Shi, P., Yin, K., Gan, J., and Qi, Y. (2004). Tides and tidal currents in the Pearl River Estuary. *Continental Shelf Res.*, 24(16):1797–1808.
- McGranahan, G., Balk, D., and Anderson, B. (2007). The rising tide: Assessing the risks of climate change and human settlements in low elevation coastal zones. *Environment and Urbanization*, 19(1):17–37.
- Mei, X., Zhang, M., Dai, Z., Wei, W., and Li, W. (2019). Large addition of freshwater to the tidal reaches of the yangtze(changjiang) river. *Estuaries & Coasts*, 42:629–640.
- Nguyen, T. T. N., Némery, J., Gratiot, N., Strady, E., Tran, V. Q., Nguyen, A. T., Aimé, J., and Payne, A. (2019). Nutrient dynamics and eutrophication assessment in the tropical riversystem of Saigon – Dongnai (southern Vietnam). *Science Total Environment*, 653:370–383.
- Petersen-Overleir, A. and Reitan, T. (2009). Bayesian analysis of stage-fall-discharge models for gauging stations affected by variable backwater. *Hydrological Processes*, 23(21):3057–3074.

- Rantz, S. E. (1963). An empirical method of determining momentary discharge of tide-affected streams. Water-Supply Paper 1586-D, U. S. Geological Survey, Washington, USA. 33 p.
- Rantz, S. E. (1982). Measurement and computation of streamflow: Volume 2. Computation of discharge. Water-Supply Paper 2175, U. S. Geological Survey. 313 p.
- Ruhl, C. A. and DeRose, J. B. (2004). Monitoring alternatives at the Sacramento River at Freeport, California: results of the 2002–2004 pilot study. Technical Report Scientific Investigation Report 2004–5172, U. S. Geological Survey, Reston, Virginia.
- Ruhl, C. A. and Simpson, M. (2006). Computation of discharge using the index-streamflow: method in tidally affected areas. Technical Report Scientific Investigations Report 2005–5004, U. S. Geological Survey, Reston, Virginia.
- Sassi, M. G. and Hoitink, A. J. F. (2013). River flow controls on tides and tide-mean water level profiles in a tidal freshwater river. *Journal of Geophysical Research*, 118:4139–4151.
- Sassi, M. G., Hoitink, A. J. F., Vermeulen, B., , and Hidayat (2011). Discharge estimation from H-ADCP measurements in a tidal river sub-

- ject to sidewall effects and a mobile bed. *Water Resources Research*, 47(W06504):1–14.
- Scussolini, P., Tran, T. T. V., Koks, E., Diaz-Loaiza, A., Ho, P. L., and Lasage, R. (2017). Adaptation to sea level rise: A multidisciplinary analysis for ho chiminh city, vietnam. *Water Resources Research*, 53:10,841–10,857.
- Taniguchi, M., Allen, D., and Gurdak, J. (2013). Optimizing the water-energy-food nexus in the Asia-Pacific Ring of Fire. *Eos, Transactions of the American Geophysical Union*, 94(47).
- Thi Ha, D., Ouillon, S., and Van Vinh, G. (2018). Water and suspended sediment budgets in the Lower Mekong from high-frequency measurements (2009–2016). *Water*, 10(7, 846):1–24.
- Thirumalai, K., DiNezio, P. N., Okumura, Y., and Deser, C. (2017). Extreme temperatures in Southeast Asia caused by El Niño and worsened by global warming. *Nature Communications*, 8(15531).
- Vachaud, G., Quertamp, F., Phan, T. S. H., Tran Ngoc, T. D., Nguyen, T., Luu, X. L., Nguyen, A. T., and Gratiot, N. (2019). Flood-related risks in ho chi minh city and ways of mitigation. *Journal of Hydrology*, 573:1021–1027.

Van, T. P. and Koontanakulvong, S. (2018). Groundwater and river interaction parameter estimation in Saigon River, Vietnam. *Engineering Journal*, 22(1):257–267.

van Driel, W. F., van, Bucx, T., Makaske, A., van de Guchte, C., van der Sluis, T., Biemans, H., Ellen, G. J., van Gent, M., Prinsen, G., and Adriaanse, B. (2015). Vulnerability assessment of deltas in transboundary river basins. techreport Report 9, Delta Alliance International, Wageningen-Delft, The Netherlands. Delta Alliance contribution to the Transboundary Water Assessment Program, River Basins Assessment.

Van Leeuwen, C. J., Dan, N. P., and Dieperink, C. (2016). The challenges of water governance in Ho Chi Minh City. *Integrated Environmental Assessment & Management*, 12(2):345–352.

Zhao, J., Chen, Z., Zhang, H., and Wang, Z. (2016). Multiprofile discharge estimation in the tidal reach of Yangtze Estuary. *Journal of Hydraulic Engineering*, 142(12, 04016056):1–12.

## **Appendix A. Sensitivity analysis**

### *Appendix A.1. Error calculation on experimental data*

A first sensitivity analysis was made to optimize main model parameters (Strickler coefficient  $K$  and the time shift  $\Delta t$ ) to experimental data. For

both ADCP campaigns in September 2016 and March 2017 (see Figure 3), the estimation of the error was made using the mean square error :

$$E(Q) = \sqrt{\frac{1}{n} \sum_{i=1}^n [Q_{mod.}(t_i) - Q_{meas.}(t_i)]^2} \quad (\text{A.1})$$

where  $n$  is the number of gauging data,  $Q_{mod.}$  the modelled discharge and  $Q_{meas.}$  the measured discharge, and  $t_i$  the time of each of these gauging. As can be observed in Fig. A.11, errors are significantly smaller for the first campaign for which the tide was more symmetrical. Indeed,  $E(Q) \approx 200 \text{ m}^3/\text{s}$  for the September 2016 campaign whereas  $E(Q) \approx 350 \text{ m}^3/\text{s}$  for the March 2017 campaign. From this sensitivity analysis, one would choose  $K = 25 \text{ m}^{1/3}/\text{s}$  and  $\Delta t = -2.04 \text{ h}$ .

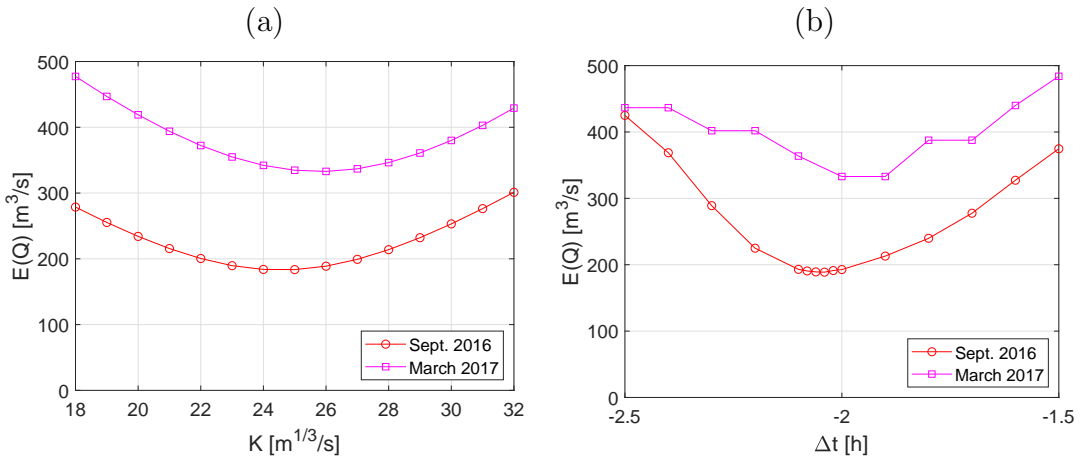


Figure A.11: Sensitivity of the Strickler coefficient  $K$  (a) and time shift  $\Delta t$  (b) on the error calculation compared to ADCP campaigns.

However, as can be seen in Figure A.12a, using  $K = 25 \text{ m}^{1/3}/\text{s}$  would

lead to some underestimation of the peak discharge values. Indeed, the error calculation is biased by the more numerous data points around the zero discharge value, which are slightly better predicted using a smaller value of the Strickler coefficient (see also Figure 3). Also, the effect of  $\Delta t$  appears not as sensitive. It is also important to realize that water level data present a frequency of 10 min (1 min in September 2016), which does not allow to fit  $\Delta t$  in such detail. Moreover, the position of the Thao Dien station (used for the 2017-2018 period) being a few km upstream of Bach Dang (used during the September 2016 experiment, see Figure reffig:Saigon), the time shift should be smaller. As a consequence, we eventually chose  $K = 26 \text{ m}^{1/3}/\text{s}$  and  $\Delta t = -2.0 \text{ h}$ .

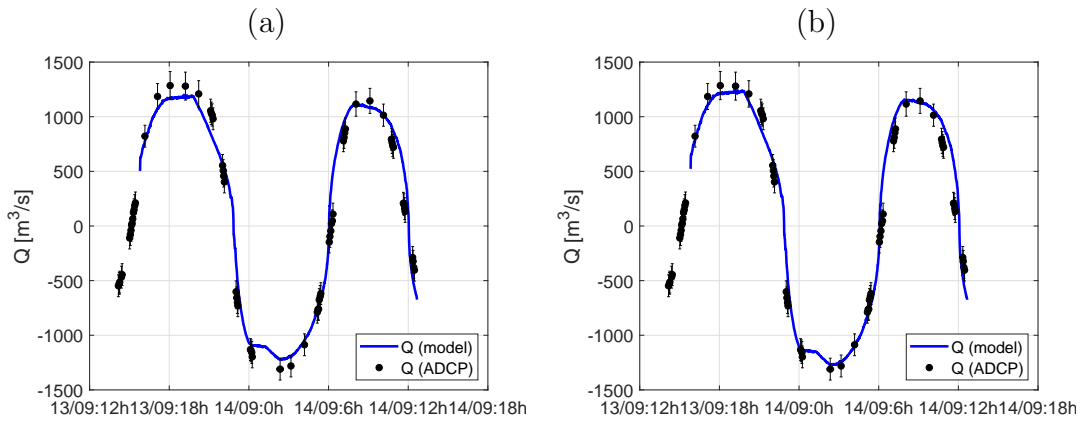


Figure A.12: Comparison between the model and discharge measurement campaigns in September 2016 using  $K = 25 \text{ m}^{1/3}/\text{s}$  and  $\Delta t = -2.00 \text{ h}$  (a) and  $K = 26 \text{ m}^{1/3}/\text{s}$  and  $\Delta t = -2.04 \text{ h}$ (b).

Appendix A.2. Sensitivity analysis on main parameters

Equation (2) was calibrated by fitting two parameters: the Strickler coefficient  $K$  and the time shift  $\Delta t$ . As can be observed in Figure A.13, the Strickler coefficient has a linear effect on both instantaneous and net discharge. It is quite obvious since  $Q \propto K$ . An error of approximately 8% in  $K$  would yield an error of 8% as well for both instantaneous and net discharge.

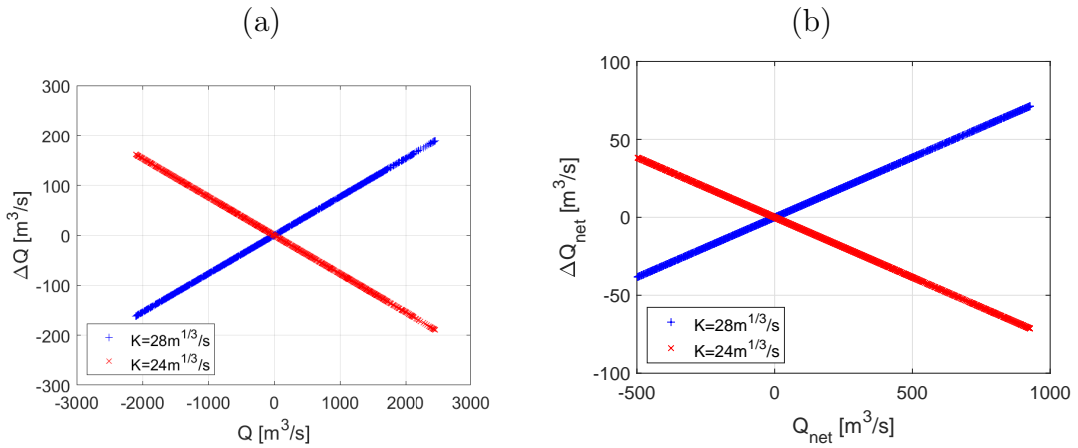


Figure A.13: Sensitivity of the Strickler coefficient  $K$  on the instantaneous (a) and net (b) discharge.

Since the coefficient  $\Delta t$  leads to a time shift of the curves, it induces large errors around the flow reverse (Figure A.14). However, the effect on the net discharge is very low; a shift of 12 min leads to an error of  $\pm 5$  m<sup>3</sup>/s approximately.

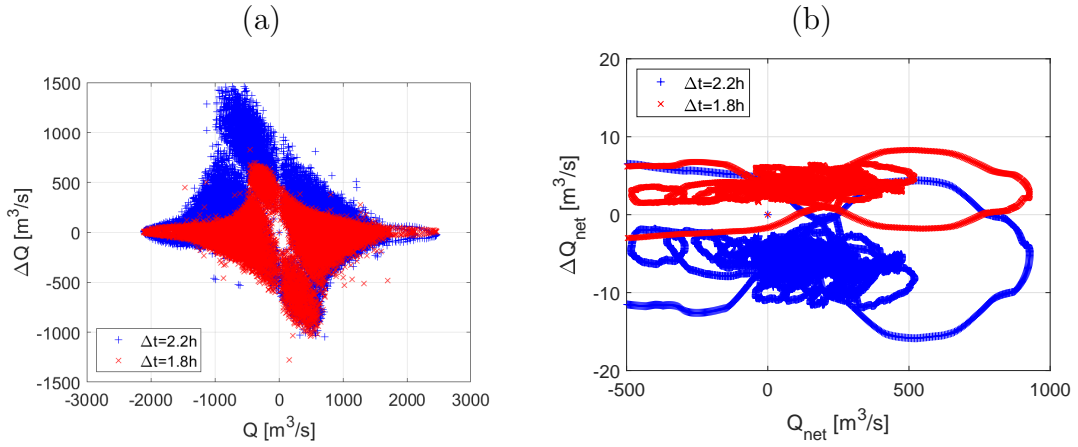


Figure A.14: Sensitivity of the time shift  $\Delta t$  on the instantaneous (a) and net (b) discharge.

### *Appendix A.3. Sensitivity analysis on input*

The only input data of the model (Equation (2)) are the water levels measured at the downstream and upstream stations. The water level measured downstream will only affect the slope estimation whereas the water level upstream (at the reference station PC) will also affect the estimation of the wet section and hydraulic radius.

In Figure A.15 is tested an error of 1 cm in the downstream water level on the estimated discharge. The effect is inversely proportional to the discharge and errors can reach  $300 \text{ m}^3/\text{s}$  for  $Q(t) \approx 0$  assuming an error of 1 cm. The asymmetrical shape of the figure is due the the time shift on the slope. On the other hand, error on the net discharge is quite limited but not negligible with an error of  $\pm 20 \text{ m}^3/\text{s}$  approximately.



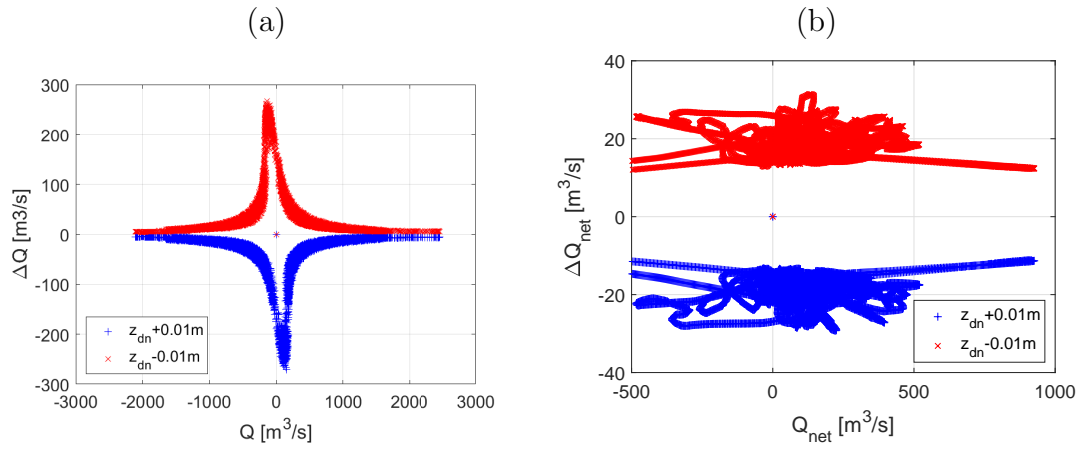


Figure A.15: Sensitivity of the water level measured downstream on the instantaneous (a) and net (b) discharge.

In Figure A.16 is presented the errors in discharge estimations for an error of 1 cm in the upstream water level. Surprisingly, effects are very similar (opposite) to the error in the downstream water level. Indeed, the sensitivity on the water slope is much higher than the sensitivity on the hydraulic radius or wet section.

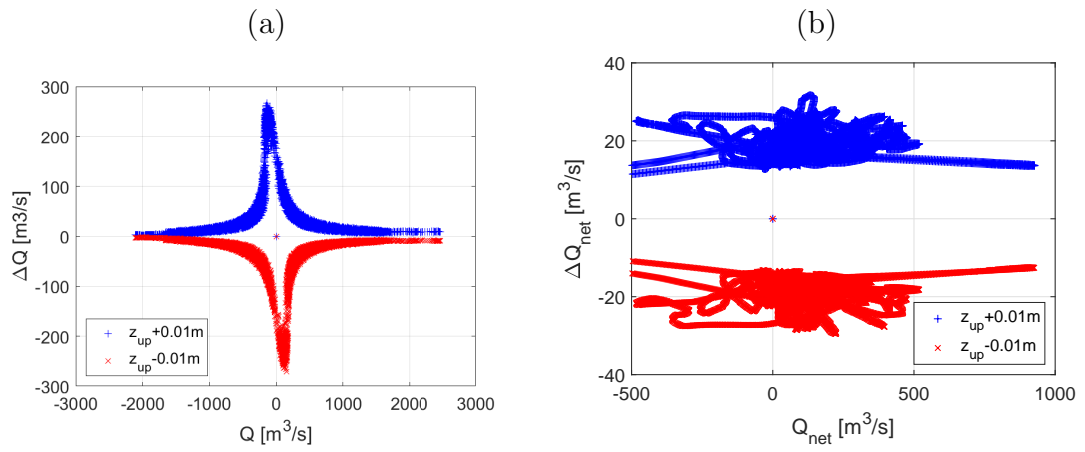


Figure A.16: Sensitivity of the water level measured upstream on the instantaneous (a) and net (b) discharge.